Progress In Electromagnetics Research Letters, Vol. 66, 121–126, 2017

Metamaterial Tri-Band Bandpass Filter using Meander-Line with Rectangular-Stub

Ashish Kumar, Dilip Kumar Choudhary, and Raghvendra Kumar Chaudhary*

Abstract—In this paper, a new compact tri-band bandpass metamaterial (MTM) filter based on meander line with a rectangular stub is proposed and designed. The pseudo connections between meander line and ports generate interdigital capacitor (IDC) to provide series capacitance. Meander line with a rectangular stub realizes a virtual ground concept here. To validate the MTM property of the proposed filter structure, a dispersion diagram is plotted. The proposed filter offers measured first passbands from 1.88–4.0 GHz; second band starts from 5.4–5.9 GHz; third passband ranges from 7.1–7.4 GHz. It has insertion losses of 0.8 dB, 1.5 dB and 2.0 dB at 2.1 GHz, 5.7 GHz and 7.3 GHz centre frequencies, respectively. The designed filter will cover S band (2–4 GHz), ISM band (5.725–5.875) and fixed satellite services (7.25–7.3 GHz). Further, the designed filter shows electrical size of $0.14\lambda_0 \times 0.13\lambda_0$ at zeroth order resonance (ZOR) frequency 2.1 GHz.

1. INTRODUCTION

In present era, the demand for reduced size and multi-functionality devices is increasing in communication systems where multiband compact bandpass filter is one of the more convincing solutions [1–9]. Various concepts and techniques have been proposed to design multiband bandpass filters such as cascading resonators [1], multi-layered structure [2], step impedance resonator [3], stub-loaded resonator [4], and MTM inspired structure [5]. The design of a multi-bandpass filter using MTM concept is a potential alternative and offers improved insertion loss, 3-dB fractional bandwidth (FBW), improved selectivity and compact size [5–7]. For these reasons, filters based on metamaterial concept have gained significant popularity, hence several filter designs based on metamaterial have been proposed [5]. An open stub-loaded resonator was discussed for designing a dual-band filter [6, 7]. Further open and short stubs loaded resonators are combined to design a triple-band filter [8, 9].

Metamaterial (MTM) is an artificial material which was first theoretically explained by Russian physicist Viktor Veselago in 1968 [10]. It supports anti-parallel phase and group velocity which produces backward electromagnetic wave [11]. In addition to this, MTM offers unique property called zeroth order (ZOR) to realize compact resonator [12].

In this paper, a new tri-band bandpass filter using meander line open stub with virtual ground concept is proposed. Meander line with a rectangular stub acts as a resonator and connected virtually to generate series capacitance C_L. The proposed filter passbands range from 1.88 to 4.0 GHz, 5.4 to 5.9 GHz and 7.1 to 7.4 GHz with maximum insertion losses of 0.8 dB (at 2.1 GHz), 1.5 dB (at 5.7 GHz) and 2.0 dB (at 7.3 GHz), respectively. Electrical size of the designed filter is $0.14\lambda_0 \times 0.13\lambda_0$ at zeroth order resonance (ZOR) frequency of 2.1 GHz, where λ_0 is free space wavelength.

Received 31 December 2016, Accepted 1 March 2017, Scheduled 10 March 2017

* Corresponding author: Raghvendra Kumar Chaudhary (raghvendra.chaudhary@gmail.com).
The authors are with the Department of Electronics Engineering, Indian Institute of Technology (Indian School of Mines), Dhanbad, Jharkhand 826004, India.

2. DESIGN AND ANALYSIS OF PROPOSED TRI-BAND BANDPASS FILTER

The proposed filter layout with design parameters and equivalent circuit are shown in Fig. 1 and Fig. 2.

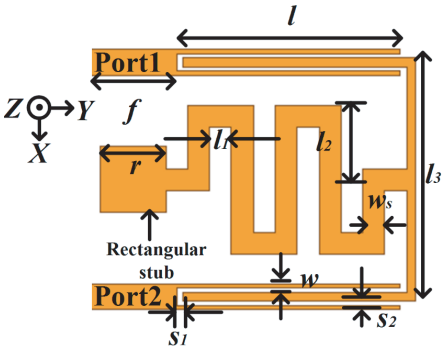

Figure 1. Proposed tri-band bandpass filter (with dimensions are in mm: $ws = 1.0$, $w = 0.2$, $l = 10.2$, $l1 = 1.0$, $l2 = 3.4$, $l3 = 11.1$, $s1 = 0.3$, $f = 4.0$, $s2 = 0.2$, $r = 3.0$).

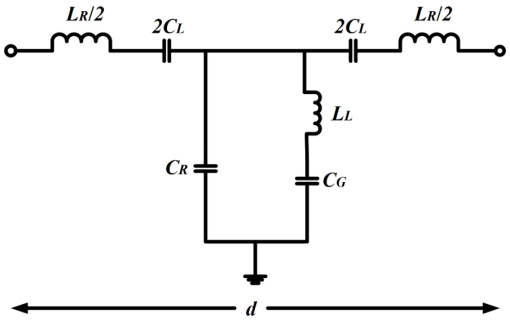

Figure 2. Equivalent circuit diagram of proposed tri-band bandpass filter.

The filter is constructed using meander line with a metal patch to realize the virtual ground concept and coupled in pseudo-interdigital format to input and output ports. This pseudo connection provides series capacitance C_L, and the current flowing through it induces magnetic flux which generates unavoidable parasitic inductance L_R. The existing voltage difference between upper and lower plates causes shunt capacitance C_R. The connected meander line in shunt will provide shunt inductance L_L, and the rectangular stub which will act as virtual ground will provide shunt capacitance of C_G to ground. Applying the Bloch-Floquet theorem [13] on obtained $ABCD$ matrix of the proposed equivalent circuit, a dispersion diagram can be obtained as

$$\cos^{-1}(\beta(\omega)d) = (1 + Y(\omega)Z(\omega)) \tag{1}$$

$$\cos^{-1}(\beta(\omega)d) = \left(1 - \left(\frac{L_L C_R}{L_L C_L} + \frac{C_G - L_R C_L^2}{L_R C_L^2 (1 - \omega^2 L_L C_G)} - \omega^2 L_L C_R\right)\right) \tag{2}$$

$$\cos^{-1}(\beta(\omega)d) = \left(1 - \left(\frac{\omega_L^2}{\omega_{Sh}^2} - \frac{\omega^2}{\omega_R^2} + \frac{\omega_L^2\omega_{Se}^2 - \omega^2\omega_G^2}{\omega_G^2 - \omega^2}\right)\right) \tag{3}$$

where $Z(\omega) = \frac{1}{j\omega C_L} + j\omega L_R$, $Y(\omega) = \frac{1}{(j\omega L_L + \frac{1}{j\omega C_G})} + j\omega C_R$, $\omega_L^2 = \frac{1}{L_L C_L}, \omega_{Sh}^2 = \frac{1}{L_L C_R}$, $\omega_G^2 = \frac{1}{L_L C_G}$ and $\omega_{Se}^2 = \frac{1}{L_R C_L}$.

As the proposed structure is open end, shunt frequency influence will be more. The input impedance for transmission line (TL) can be obtained from Eq. (4) as

$$Z_{in} = Z_0 \left(\frac{Z_L + jZ_0 \tan(\beta d)}{Z_0 + jZ_L \tan(\beta d)}\right) \tag{4}$$

For open ended structure the input impedance becomes

$$Z_{in}|^{Z_L \to \infty} = -jZ_0 \cot(\beta d) \tag{5}$$

The ZOR input impedance (Z_{in}^{open}) seen from one end to another of the proposed structure is given as

$$Z_{in}^{open} = -jZ_0 \cot(\beta d)^{\beta \to 0} = -jZ_0 \frac{1}{\beta d} \tag{6}$$

$$= -j\sqrt{\frac{Z'(\omega)}{Y'(\omega)}} \left(\frac{1}{d \times -j\sqrt{Z'(\omega)Y'(\omega)}}\right) = \frac{1}{Y'(\omega)d} = \frac{1}{Y} \tag{7}$$

where Z' and Y' are impedance and admittance per unit cell, and d is length of designed filter. Eq. (7) shows that open-ended case input impedance depends on resonance of shunt impedance. Thus, ZOR frequency (ω_{ZOR}) of an open-ended case can depend on lumped value of shunt tank resonator circuit and can be calculated as

$$\omega_{ZOR} = \sqrt{\frac{1}{L_L C_R}} \tag{8}$$

To validate the MTM properties (backward wave propagation, anti-parallel phase and group velocity, dispersion diagram), a dispersion diagram is plotted for the proposed structure. The dispersion diagram of the proposed tri-band bandpass filter can be obtained by Eq. (9) as shown below

$$\beta = \frac{1}{d}\left(\frac{1 - S_{11}S_{22} + S_{12}S_{21}}{2 \times S_{21}}\right) \tag{9}$$

The dispersion diagram of the designed filter by using Eq. (9) is shown in Fig. 3. It shows that extension of the first band has both negative and positive slopes, which confirms it as composite right/left-handed (CRLH) band. The second band extends from 5.4 to 5.9 GHz with negative slope, which validates it as LH band. The third band is RH band, and its band ranges from 7.1 to 7.4 GHz.

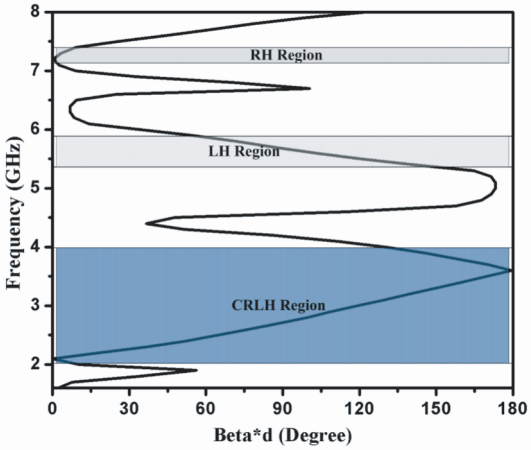

Figure 3. Dispersion diagram for proposed triple band bandpass filter.

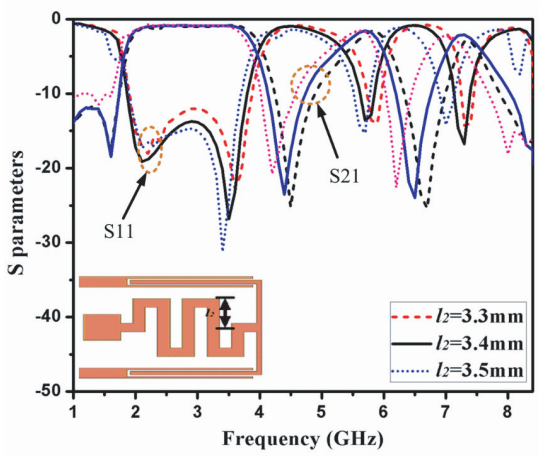

Figure 4. Effect on S-parameters with different length of meander line.

Transition time of a signal across a design is defined by group delay (t_{gd}). This can be calculated as negative slope of insertion phase response with respect to frequency [14].

$$t_g = -\frac{\partial \phi_{S_{21}}}{\partial \omega} \tag{10}$$

where $\phi_{S_{21}}$ is the phase of insertion loss in radian and ω the angular frequency. It is clear from above analysis that shunt frequencies of proposed filter can be controlled by tuning the length of meander line. As the length of meander line varies, the connected shunt inductance will change, hence its shunt frequencies will vary, and centre frequency of designed band will vary too as shown in Fig. 4.

Centre frequencies of the proposed design are dependent on both series interdigital capacitance (IDC) and meander line shunt tank resonator. The contribution of IDC and shunt tank circuit can be shown using surface current density, hence surface current density for the proposed filter at different frequencies is plotted and shown in Fig. 5. It depicts that ZOR frequency at 2.1 GHz is possibly affected by meander line, and resonant mode at 3.5 GHz is mainly due to the patch of length $l3$ which is connected to meander line. The second band at centre frequency of 5.7 GHz is influenced due to pseudo connection (connection between meander line and input/output ports) providing IDC. Meander line and IDC are responsible for 7.3 GHz centre frequency of the third band.

The variation of group delay with different series gaps (s_2) is shown in Fig. 6. It can also be observed that as s_2 increases, group delay increases, and average group delay is less than 0.5 ns in the proposed passbands.

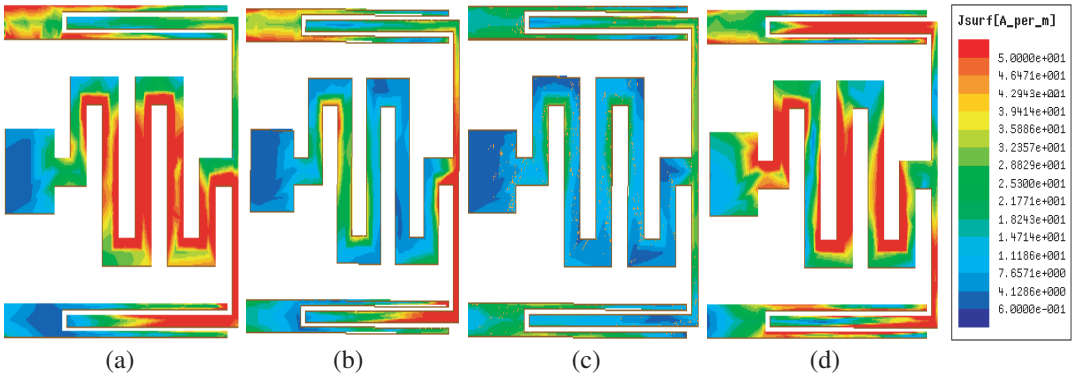

Figure 5. Surface current density on tri-band bandpass filter at different frequencies, (a) 2.1 GHz, (b) (c) 5.7 GHz, (d) 7.3 GHz.

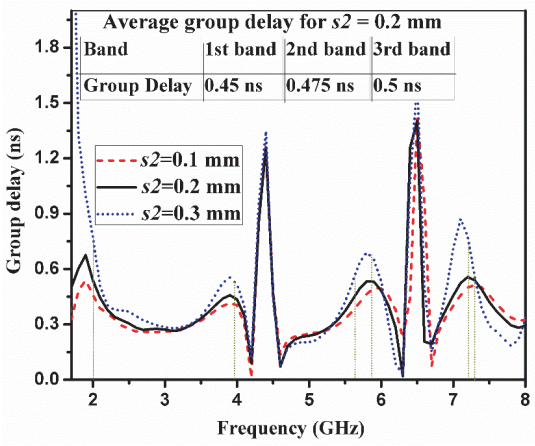

Figure 6. Variation in group delay with respect to series gap (s_2).

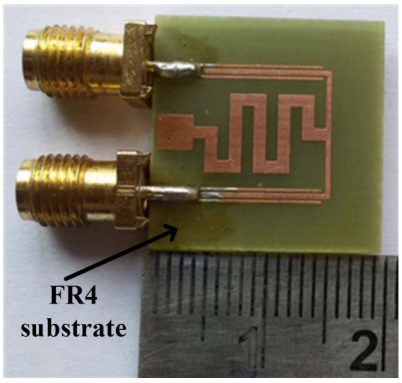

Figure 7. Photo of fabricated proposed tri-band bandpass filter.

3. EXPERIMENTAL RESULTS AND DISCUSSIONS

The proposed triple-band bandpass filter is fabricated on an FR4 substrate (with thickness of 1.6 mm, dielectric constant $\varepsilon_r = 4.4$ and loss tangent of 0.02) as shown in Fig. 7.

Agilent N5221A Vector Network Analyzer is used to measure S-parameter and group delay of the proposed tri-band bandpass filter. The measured scattering parameters and simulated result are compared in Fig. 8. The measured result shows insertion losses of 0.8 dB (at 2.1 GHz), 1.6 dB (at 5.7 GHz) and 2.4 dB (at 7.3 GHz) bandpass center frequencies. There is a slight increase in insertion loss of measured value compared to simulated due to imperfection in fabrication and substrate used.

Comparison of the measured and simulated group delays is shown in Fig. 9. It shows that measured group delay is slightly higher than the simulated result in the first passband and almost similar for the second and third passbands. Glitches observed in the group delay depict the attenuation of transmitted signal beyond passbands. Simulated result confirms that the group delay is reasonably flat over the designed passbands. The bandwidth of each passband can be controlled by varying the gap between IDCs ($s2$), which is shown in Fig. 10. By increasing the gap (s2), the bandwidth of the 1st passband increases, and those in 2nd and 3rd passbands decrease.

To justify the proposed structure, comparison of performance is made among earlier published triple band filters, as shown in Table 1. This table shows that the proposed filter has advantages of low insertion loss, high return loss, high 3 dB fractional bandwidth (FBW) and compact size. The proposed filter has electrical size of $0.14\lambda_0 \times 0.13\lambda_0$ at zeroth order resonance (ZOR) frequency 2.1 GHz, where λ_0 is free-space wavelength.

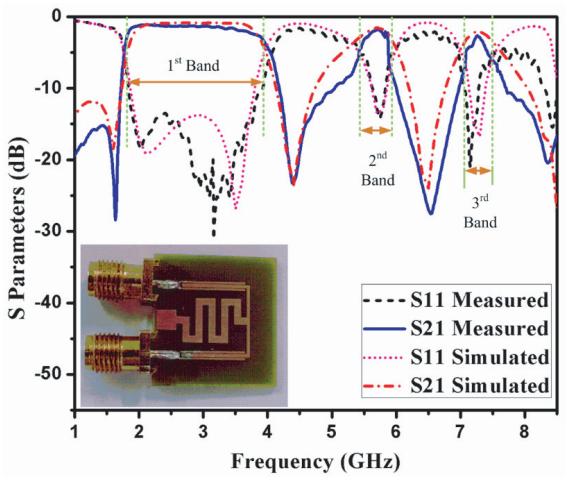

Figure 8. Simulated and measured scattering parameters of proposed tri-band bandpass filter.

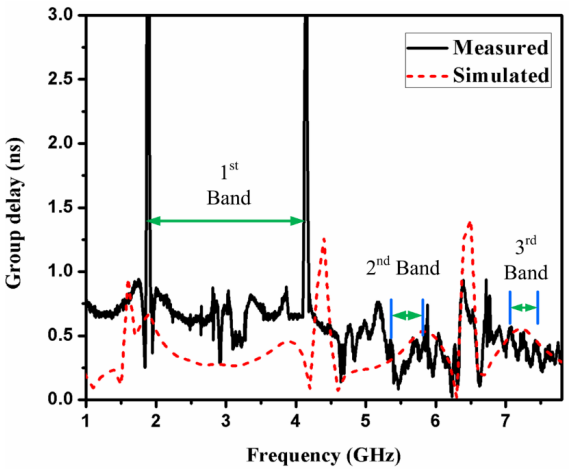

Figure 9. Simulated and measured group delay of designed tri-band bandpass filter.

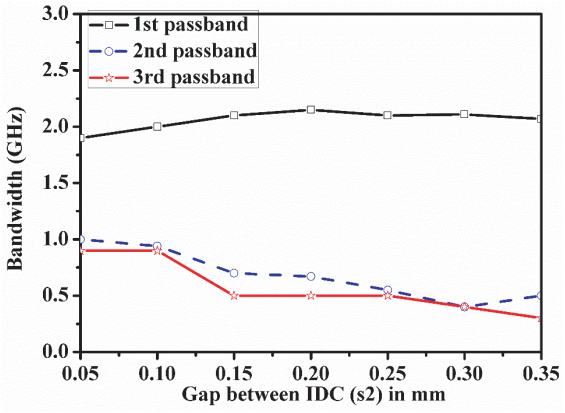

Figure 10. Variation in bandwidth by changing the gap of C-IDC.

Table 1. Comparison with earlier published triple band bandpass filter.

Ref.	1st/2nd/3rd Passbands (GHz)	Insertion loss (dB)	Return loss (dB)	FBW (%)	Dimensions ($\lambda_0 \times \lambda_0$)
[4]	2.45/3.5/5.3	0.9/1.7/2.1	37/15/15	14/7/4	0.43×0.53
[7]	1.575/2.4/3.5	1.6/1.5/2.3	9/18.9/13.5	5.2/3.8/4.6	0.72×0.82
[15]	2.4/3.5/5.2	1.9/1.4/1.5	14/15/17	6/12/12	0.23×0.13
[16]	2.45/3.5/5.25	2/2.4/1.7	18/16/13	2.5/1.7/5	0.19×0.18
[17]	3.48/4.18/5.52	1.53/2.11/2.65	15.1/22.8/19	7/5/6	0.21×0.11
[18]	1.37/2.43/3.53	1.7/1.8/2.5	20/15/22	4.4/5.9/2.7	0.18×0.10
This work	2.1/5.7/7.3	0.8/1.6/2.4	25.5/15/23	57.1/8.7/4.1	0.14×0.13

4. CONCLUSION

A new compact tri-band bandpass metamaterial filter based on meander line open stub with a virtual short resonator is designed. The designed filter has three passbands in 1.88–4 GHz, 5.4–5.9 GHz and 7.1–7.4 GHz. The measured insertion losses within these passbands are 0.8 dB, 1.6 dB and 2.4 dB. A sharp attenuation of more than 25 dB is obtained between the passbands. The return losses are 25.5 dB, 15 dB and 23 dB at center frequencies of the proposed passbands, respectively. The simulated result of the proposed filter design is compared with experimental result, and good agreement is found. It has

compact electrical size of $0.14\lambda_0 \times 0.13\lambda_0$ at ZOR frequency. The proposed tri-band bandpass filter may have application inWLAN/WiFi, WiMAX, ISM band and fixed satellite service.

REFERENCES

1. Chen, C., T. Huang, and R. Wu, "Design of dual and triple-passband filters using alternately cascaded multiband resonators," *IEEE Transactions on Microwave Theory and Techniques*, Vol. 54, 3550–3558, 2006.
2. Weng, M., H. Wu, K. Shu, J. Chen, R. Yang, and Y. Su, "A novel triple-band bandpass filter using multilayer-based substrates for WiMAX," *37th European Microwave Conference*, 325–328, 2007.
3. Chu, Q. X. and X. M. Lin, "Advanced triple-band bandpass filter using tri-section SIR," *Electronics Letter*, Vol. 44, 295–296, 2008.
4. Lai, X., C. H. Liang, H. Di, and B. Wu, "Design of tri-band filter based on stub loaded resonator and DGS resonator," *IEEE Microwave and Wireless Components Letters*, Vol. 20, 265–267, 2010.
5. Fouad, M. A. and M. A. Abdalla, "New π-T generalised metamaterial negative refractive index transmission line for a compact coplanar waveguide triple band pass filter applications," *IET Microwave and Antennas Propagation*, Vol. 8, 1097–1104, 2014.
6. Zhang, X. Y., J. X. Chen, and X. Quan, "Dual-band bandpass filter using stub-loaded resonators,"*IEEE Microwave and Wireless Components Letters*, Vol. 17, 583–585, 2007.
7. Chen, W., M. Weng, and S. Chang, "A new tri-band bandpass filter based on stub-loaded step-impedance resonator," *IEEE Microwave and Wireless Components Letters*, Vol. 22, 179–181, 2012.
8. Chen, F. C., Q. X. Chu, and Z. H. Tu, "Tri-band bandpass filter using stub loaded resonators," *Electronics Letter*, Vol. 44, 295–296, 2008.
9. Chen, J., Y. She, H. Wang, Y. Liu, and N. Wang, "Design of compact tri-band filter based on SIR-loaded resonator with 0° feed," *IEEE International Conference on Communication Problem-Solving*, 322–325, Beijing, 2014.
10. Veselago, V., "The electrodynamics of substances with simultaneously negative values of ε and μ," *Soviet Physics Uspheki*, Vol. 10, 509–514, 1968.
11. A. K. Iyer, and G. V. Eleftheriades, "Negative refractive index metamaterials supporting 2-D waves," *Int. Microwave Symp.*, Vol. 2, 1067–1070, June 2002.
12. Caloz, C. and T. Itoh, *Electromagnetic Metamaterials: Transmission Line Theory and Microwave Applications*, John Wiley & Sons, Inc., 2006.
13. Sanada, A., K. Murakami, S. Aso, H. Kubo, and K. Awai, "A via-free microstrip left-handed transmission line," *Microwave Symposium Digest*, Vol. 1, 301–304, 2004.
14. *Technical Note on Network Analyzer Basics*, Agilent Technologies, USA, http://cp.literature.agilent.com/litweb/pdf/5965-7917E.pdf.
15. Chu, Q. X., X. H. Wu, and F. C. Chen, "Novel compact tri-band bandpass filter with controllable bandwidths," *IEEE Microwave and Wireless Components Letters*, Vol. 21, 655–657, 2011.
16. Chen, F. C. and Q. X. Chu, "Design of compact tri-band bandpass filters using assembled resonators," *IEEE Transactions on Microwave Theory and Techniques*, Vol. 57, 165–171, 2009.
17. Mo, Y., K. Song, and Y. Fan, "Miniaturized triple-band bandpass filter using coupled lines and grounded stepped impedance resonators," *IEEE Microwave and Wireless Components Letters*, Vol. 24, 333–335, 2014.
18. Lan, S., M. Weng, S. Chang, C. Hung, and S. Liu, "A tri-band bandpass filter with wide stopband using asymmetric stub-loaded resonators," *IEEE Microwave and Wireless Components Letters*, Vol. 25, 19–21, 2015.